Through-plane dark-rim artefacts in 3D first-pass perfusion

Merlin J Fair[1,2], Peter D Gatehouse[1,2], and David N Firmin[1,2]
[1]NHLI, Imperial College London, London, United Kingdom, [2]NIHR Cardiovascular BRU, Royal Brompton Hospital, London, United Kingdom

Background: The dark-rim artefact (DRA) is well known in 2D first-pass perfusion (FPP). While the in-plane features of DRAs are understood, this effect along the second phase-encoding (partition) direction used for 3D imaging has not yet been examined. The Gibbs contribution to DRAs in 2D FPP is minimised by finer resolution [1], but the low through-plane resolutions currently achievable in 3D FPP imply risk of partition axis DRAs. These new partition DRAs ("PDRAs") and partial volume effects due to coarse resolution of this direction were investigated.

Methods: Low-resolution data at typical 3D FPP parameters were subsampled from 3 high-resolution sources to study PDRAs. High in-plane resolution was maintained so that any changes arose only from through-plane effects. The subsampled number of partitions used in the reconstructions (Np) was varied to give a 2-32mm range of through-plane resolutions.

1. A numerical phantom modelled a conical LV at intensity ratio 5:2 (blood:myocardium at first pass peak). Np, and the angle between endocardial wall and image plane, θ_B, were varied while plotting width of PDRAs.
2. In-vivo investigation: single-frame high-resolution data (1.3x1.3x2.0mm) was acquired by navigator-gated bSSFP at high flip-angle for similar blood:myocardium intensity ratio (approx 2:1).
3. LV blood and myocardium were manually segmented and the intensity of each tissue uniformly set to the 5:2 ratio of the numerical phantom. This gave more anatomically realistic data than the uniform cone, with changing θ_B along and around the LV, without contaminating affects from outside the LV.

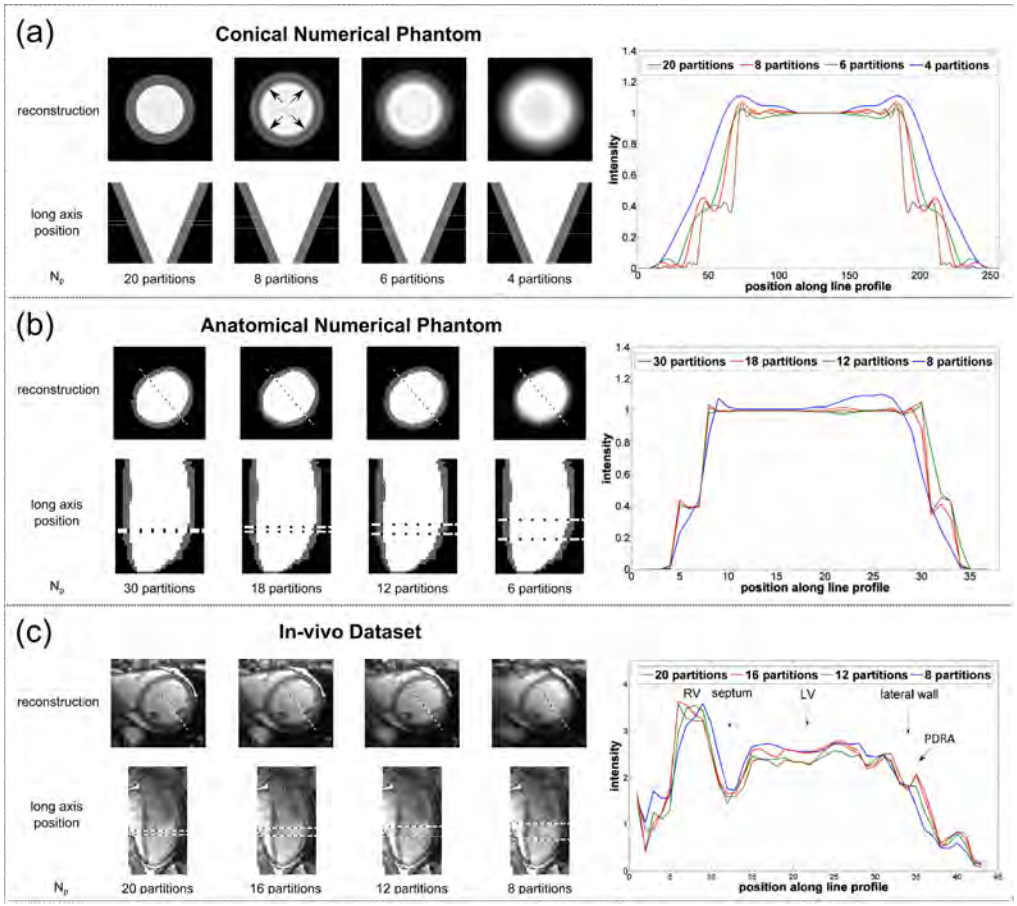

Fig 1: SAX reconstructions of 'slices' at fixed in-plane but varying through-plane resolutions, shown with their corresponding locations along the high-resolution long-axis. To their right are the corresponding line profiles. a) conical numerical phantom, b) anatomical numerical phantom and c) in-vivo dataset. N_p values chosen to give representation of small PDRA, stronger PDRA, partial-volume/PDRA compromise and strong partial-volume effects respectively from left to right.

Results: Slice reconstructions (Fig 1) show overlapping consequences of increased PDRAs and partial volume (blurring) as slice thickness is increased. Arrows (1a) show PDRA in the 8-partition image coming through-plane, n.b. not an in-plane DRA. Variation of θ_B and N_p in the conical phantom significantly altered PDRA width (Fig 2), with strongest artefacts at combined low resolution and sharp θ_B. Although the border is sharpest at θ_B near 90°, this implies no variation between planes and therefore no PDRA. Whilst PDRA width increases at coarser resolution, the simultaneous impact of partial volume at lower N_p counteracts this effect. Eventually the blurring dominates and destroys endocardial border visibility. This pattern was seen in conical and anatomical phantoms (Fig 1a&b) and to some extent in-vivo (Fig 1c), although complicated by intensity slopes and effects beyond the LV. For some values of θ_B examined (~>65°) that may well occur in-vivo, sufficiently high through-plane resolution to avoid PDRAs is infeasible in 3D FPP; however, some compromise between PDRA and partial volume may be possible.

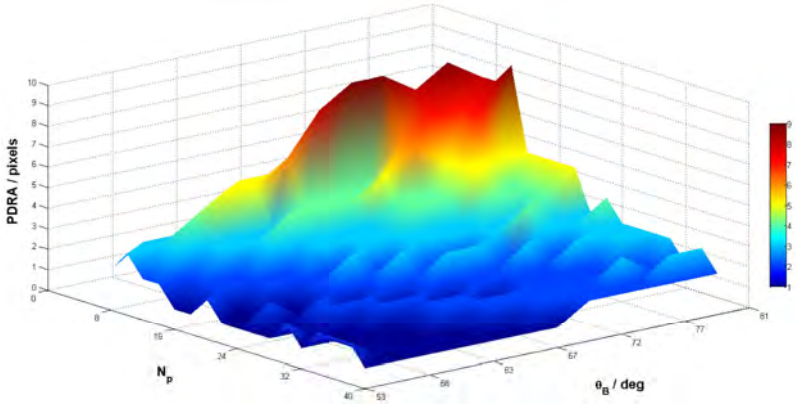

Conclusions: Contrary to expectation that increased resolution reduces DRAs, at the low through-plane resolutions available in 3D FPP finer resolution in this direction may increase Gibbs-induced DRAs due to sharper through-plane boundaries. However, this is a trade-off against partial volume effects/blurring at low partition number resolution. Further in-vivo investigations are required to optimise the compromise between these two effects.

Fig 2: Values of the PDRA width (in number of pixels) in the conical numerical phantom, reconstructed at varying boundary angles (θ_B) and number of secondary phase-encode steps (partitions) (N_p).

References: (1) Plein et al, MRM, 2007